

MTSAT Window Channels' (IR1 and IR2) Potential for Distinguishing Volcanic Ash Clouds

Masami Tokuno*

Abstract

GMS-5 infrared window channels [IR1 (10.5 - 11.5 μm) and IR2 (11.5 - 12.5 μm)] have been successfully used to distinguish volcanic ash clouds from water/ice clouds. Results for the Brightness Temperature Difference (BTD) of the two channels become negative for volcanic ash clouds and positive for ice/water clouds. The response functions of IR1 (10.3 - 11.5 μm) and IR2 (11.5 - 12.5 μm) for the Multi-functional Transport Satellite (MTSAT), a successor to GMS-5, have been significantly improved. Therefore, this research has documented the improvement in discrimination of volcanic ash clouds and meteorological clouds using two-channel data in the thermal infrared spectrum based on results derived from a radiative transfer model. Radiative transfer calculations have been made with a semitransparent cloud model based on assumptions of a spherical particle shape, a homogeneous underlying surface, and a simple thin cloud parallel to the surface. To evaluate the temperature difference between two window channels caused by the difference in the two response functions, the BTD value was determined between two infrared window channels using MTSAT, GMS-5, and NOAA-14/AVHRR to observe quartz (volcanic ash cloud) and ice (meteorological high level cloud). Calculations were made with assumptions that: (1) the vertical profile of the atmosphere is the tropical, the midlatitude summer, and the midlatitude winter atmospheric model, (2) the cloud base height is 10 km for the midlatitude summer and winter atmospheric models, and 14 km for the tropical model over the surface while geometrical cloud thickness is 1 km, (3) a modified- γ size distribution is used and the satellite optical cloud thickness is varied from 0 to 9 by changing the total number of particles per unit of volume. The results indicate that the BTD value is greatest for MTSAT, lesser for NOAA-14/AVHRR, and lowest with GMS-5 for every case in the study. For example, given a mode particle radius of 2 μm and satellite cloud optical depth of 3.0 in the tropical atmospheric model, the BTD value is -25K for MTSAT, -22K for NOAA-14/AVHRR, and -16K for GMS-5. Thus, results confirm that MTSAT data can further improve the detection of volcanic ash clouds in relation to images from GMS-5.

*Meteorological Satellite Center, System Engineering Division

(Received August 6, 1999 : Revised November 24, 1999)

1. Introduction

NOAA AVHRR window channels [channels 4 (10.5 - 11.5 μm) and 5 (11.5 - 12.5 μm)] have been successfully used to distinguish volcanic ash clouds from water/ice clouds in work by Prata (1989) and Potts (1993) based on the fact that the Brightness Temperature Difference (BTD) of two channels becomes negative for volcanic ash clouds and positive for ice/water clouds. Also, GMS-5 window channels IR1 and IR2 have been used to detect and monitor volcanic ash clouds, as proven by Tokuno (1997). However, GMS-5 infrared data is digitized only to eight bits and some overlap occurs in spectral response functions for GMS-5 infrared sensors IR1 and IR2, which produced a reduced BTD for GMS-5 when compared to that for NOAA AVHRR.

The Multi-functional Transport Satellite (MTSAT) is a successor to GMS-5 that will be launched in 2002 - 2003. This satellite will have one visible sensor (0.55 - 0.8 μm) and four infrared sensors (IR1: 10.3 - 11.3 μm; IR2: 11.5 - 12.5 μm; IR3: 6.5 - 7.0 μm; IR4: 3.5 - 4.0 μm). Infrared data will be digitized to 10 bits, significantly improving the thermal resolution. In addition, MTSAT's IR1 and IR2 do not have any overlap for spectral response functions like the GMS-5's IR1 and IR2 infrared sensors. This improvement will lead MTSAT to more effectively distinguish volcanic ash clouds than GMS-5.

The potential of MTSAT window channels to distinguish volcanic ash clouds involves an improvement of spectral response functions for IR1 and IR2 that will occur based on results from a radiative transfer model. The radiative transfer model and the Mie calculation are the

same as described by Tokuno (1997). In chapters 2 and 3, this radiative transfer model and Mie calculation have been reviewed.

The silica content of volcanic ash clouds is often high (over 50 % SiO₂), as shown by Newell and Deepak (1982), and is not present in normal water/ice clouds. Therefore, quartz has been used for volcanic ash clouds and ice for meteorological high level clouds to calculate radiance in an ideal case.

2. The Radiative Transfer Model

If there are no ice/water clouds between the surface and overlying clouds, e.g., volcanic ash cloud, the monochromatic upwelling thermal radiance observed by the satellite sensor is expressed as

$$B_{e,\nu}(\mu) = B_{s,\nu} \exp(-\tau_{\nu}/\mu) + \int_0^{\tau_{\nu}} \exp(-\tau'/\mu) S(\tau') d\tau'/\mu$$

where ν is the wavenumber, $B_{e,\nu}$ is observed radiance, $B_{s,\nu}$ is radiance reached the cloud base, τ_{ν} is the cloud optical depth at wavenumber ν , and μ is the cosine of the viewing angle. The source function $S(\tau')$ is at the optical depth τ' in the cloud. In addition, the attenuation of the upwelling thermal radiance due to the atmosphere between the satellite and the cloud is disregarded.

Based on assumptions that $S(\tau')$ is approximated by a two-stream source function and the cloud is isothermal, the equation for thermal radiance is changed by applying a technique from Ackerman et al. (1988):

$$B_{e,\nu}(\mu) = B_{s,\nu} \exp(-\tau_{\nu}/\mu) + B_{c,\nu} (1 - \exp(-\tau_{\nu}/\mu)) + B_{s,\nu} \delta_s(\mu, \tau_{\nu}) - B_{c,\nu} \delta_c(\mu, \tau_{\nu})$$

where $B_{c,\nu}$ is the radiance of a black body at a

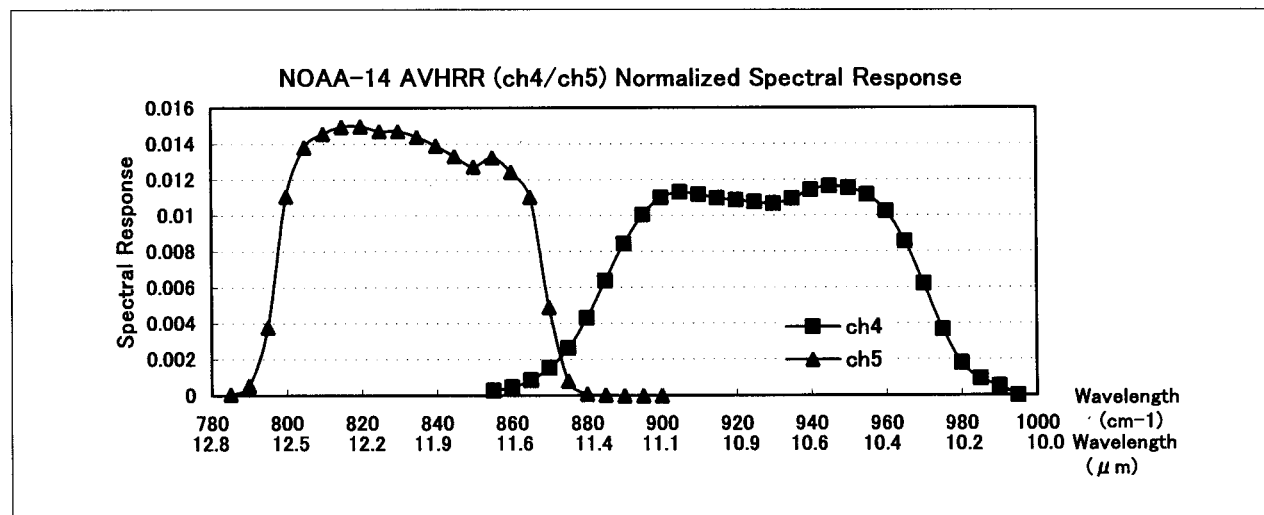
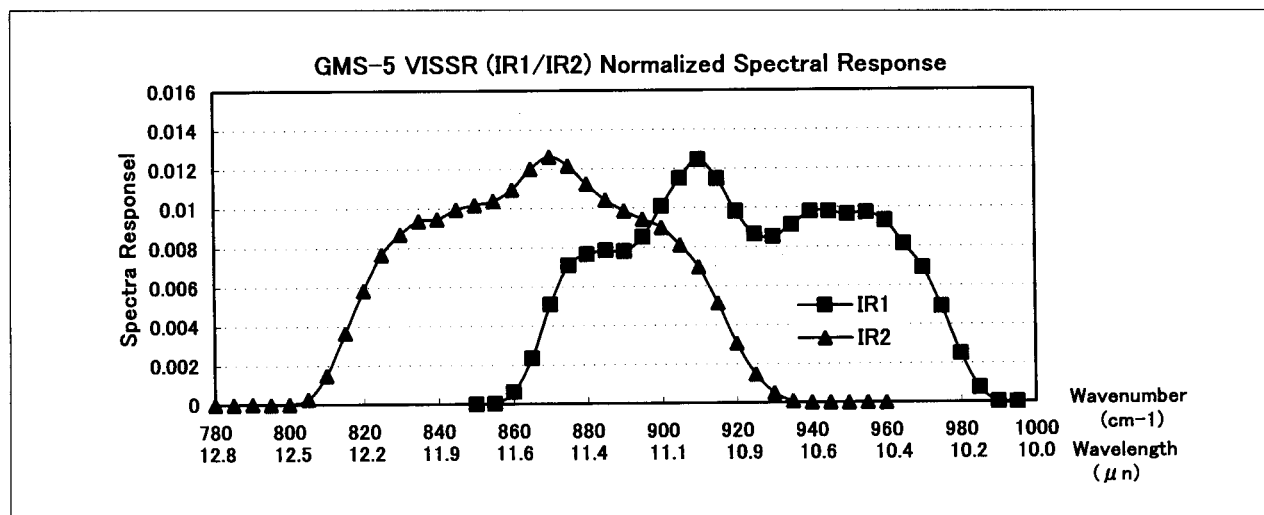
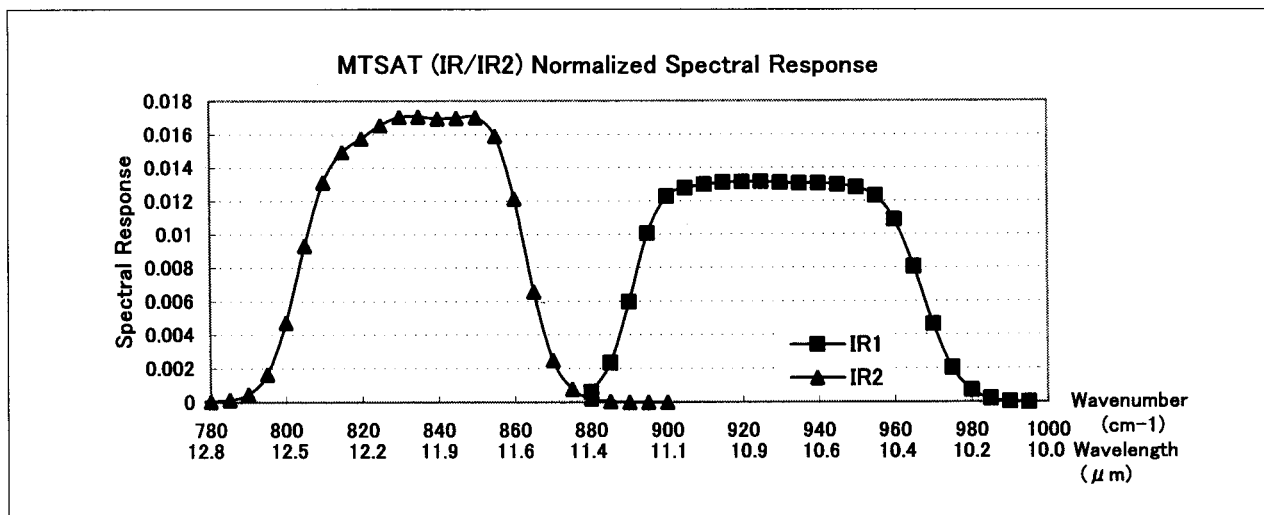


Fig. 1 Normalized response function for MTSAT thermal channels 1 and 2, GMS-5 thermal channels 1 and 2, and NOAA-14 AVHRR thermal channels 4 and 5. The spectral response at intervals of 5 cm⁻¹ is indicated by the symbols (▲ and ■).

cloud temperature with wavenumber ν . The coefficients of the last two terms are written as

$$\delta_s = (f - \Gamma^2 f^+) / 2D$$

$$\delta_c = (1 - \Gamma \exp(-\lambda \tau_c) \cdot (f^- + \exp(\lambda \tau_c) \cdot \Gamma f^+) / 2D$$

where

$$\lambda = 2(1 - \gamma)^{1/2}$$

$$\gamma = \omega_c (1 - g_c)$$

$$D = \exp(\lambda \tau_c) \cdot \Gamma^2 \exp(-\lambda \tau_c)$$

$$\Gamma = (2 - \lambda) / (2 + \lambda)$$

$$f^- = ((2 - \lambda) / (1 - \mu \lambda)) \cdot (1 - \exp(-(1 - \mu \lambda) \tau_c / \mu))$$

$$f^+ = ((2 + \lambda) / (1 + \mu \lambda)) \cdot (1 - \exp(-(1 + \mu \lambda) \tau_c / \mu))$$

Here, $\tilde{\omega}_c$ is the single-scattering albedo and g_c the asymmetry factor of the cloud layer.

Space satellite sensors are designed to measure radiance with a wavenumber range $\nu_1 < \nu < \nu_2$ but not monochromatic radiance. The observed response-weighted radiance as detected by the sensor of the satellite is therefore expressed as

$$I_{e,i}(\mu) = \int_{\nu_1}^{\nu_2} \Psi_i(\nu) B_{e,\nu}(\mu) d\nu$$

where $\Psi_i(\nu)$ is the normalized spectral response function for channel i . The normalized response function for MTSAT thermal channels 1 and 2, GMS-5 thermal channels 1 and 2, and NOAA-14 AVHRR thermal channels 4 and 5, are shown in Fig. 1.

3. Mie Calculation

To obtain the theoretical radiance defined in the altered thermal radiance equation, optical cloud properties must be entered. In this study, cloud particles are assumed to be spherical, so the Mie theory can be used to calculate the efficiency factor for extinction, scattering, or absorption; asymmetric parameters; and the single-scattering albedo for known refractive indices. These optical properties are calculated in the following equations:

Efficiency factors:

$$\hat{Q}_t = \left(\int_0^\infty \pi r^2 Q_t(2\pi r / \lambda, m) (dn(r) / dr) dr \right) / \left(\int_0^\infty \pi r^2 (dn(r) / dr) dr \right)$$

where Q_t is the Mie efficiency factor for extinction, scattering, or absorption; $n(r)$ is the size distribution of particles with radius r for the number of particles per unit volume; m values are the refractive indices; and λ is wavelength.

Extinction, absorption, and scattering efficiencies are related by

$$\hat{Q}_{\text{ext}} = \hat{Q}_{\text{abs}} + \hat{Q}_{\text{sca}}$$

The single scattering albedo is

$$\tilde{\omega} = \hat{Q}_{\text{sca}} / \hat{Q}_{\text{ext}}$$

The asymmetry parameter is

$$\hat{g} = \left(\int_0^\infty \pi r^2 Q_{\text{sca}} g(2\pi r / \lambda, m) dn(r) / (dr) dr \right) / \left(\int_0^\infty (\pi r^2 Q_{\text{sca}} dn(r) / (dr) dr \right)$$

where g is the asymmetric parameter for a single particle and Q_{sca} is the Mie efficiency factor for scattering.

The modified- γ distribution is commonly

used to model normal cloud particle distributions and has also been used to compare ash particle distributions based on the results of size spectral data from Whitten (Ed.)(1982) recorded by Mt. St. Helens for clouds at various times after three eruptions. Therefore, it is assumed that particle size distribution, $n(r)$, is the modified- γ size distribution used by Prata and Barton (1994). That is, size distribution is given by

$$dn(r)/dr = (Nb^7/6!) r^6 \exp(-br)$$

where $b = 6/r_0$, r_0 is the mode particle radius, and N is the total number of particles per unit volume.

Optical cloud thickness is calculated from the size distribution, extinction efficiency, and geometrical thickness of the cloud. These factors are related by

$$\tau_c = \hat{Q}_{ext} L \int_0^\infty (\pi r^2 dn(r)/dr) dr$$

where L is the geometrical thickness.

The scattering parameters required for radiative transfer calculations are obtained using subroutines for computing parameters of the electromagnetic radiation scattered by a sphere as developed by J.V. Dave (1968).

Figure 2 shows the refractive indices of quartz and ice in the wavelength region (10 - 13 μm) obtained from Takashima and Masuda (1987) based on data from Spitzer and Kleinman (1961) and Warren (1984).

The value for the real part of the quartz decreases in a wavelength of 11-12 μm and that for the imaginary part increases in this region. In contrast, the value for the real part of ice gradually increases in a wavelength of 11 μm and the value for the imaginary part

gradually increases in a wavelength of 10 - 11.5 μm and then becomes a constant value in a wavelength greater than 11.5 μm .

The modified- γ size distribution is used for calculations with a mode of the particle radius of 2, 3, or 5 μm . Figure 3 shows results of calculations when $r_0 = 3 \mu\text{m}$ and $N = 100 \text{ cm}^{-3}$, indicating that volcanic substances (quartz) have an extinction larger than ice and that the

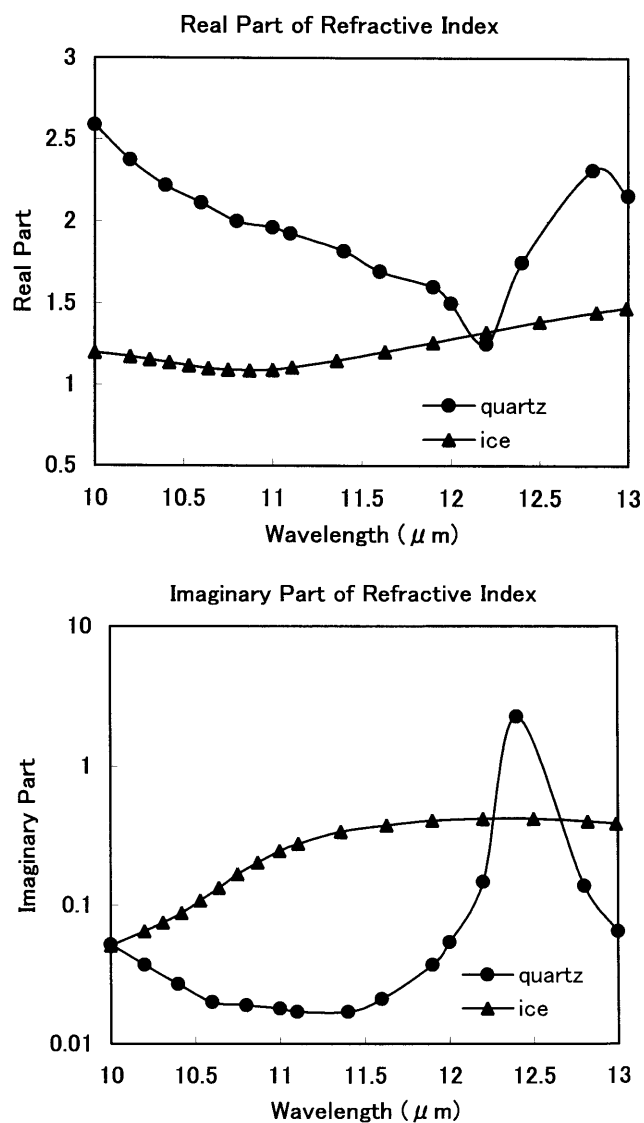


Fig. 2 The real part (upper) and imaginary part (lower) of the refractive indices for quartz (●) and ice (▲) in the wavelength region (10 - 13 μm) from Takashima and Masuda (1987) based on data by Spitzer and Kleinman (1961) and Warren (1984) [from Tokuno (1997)].

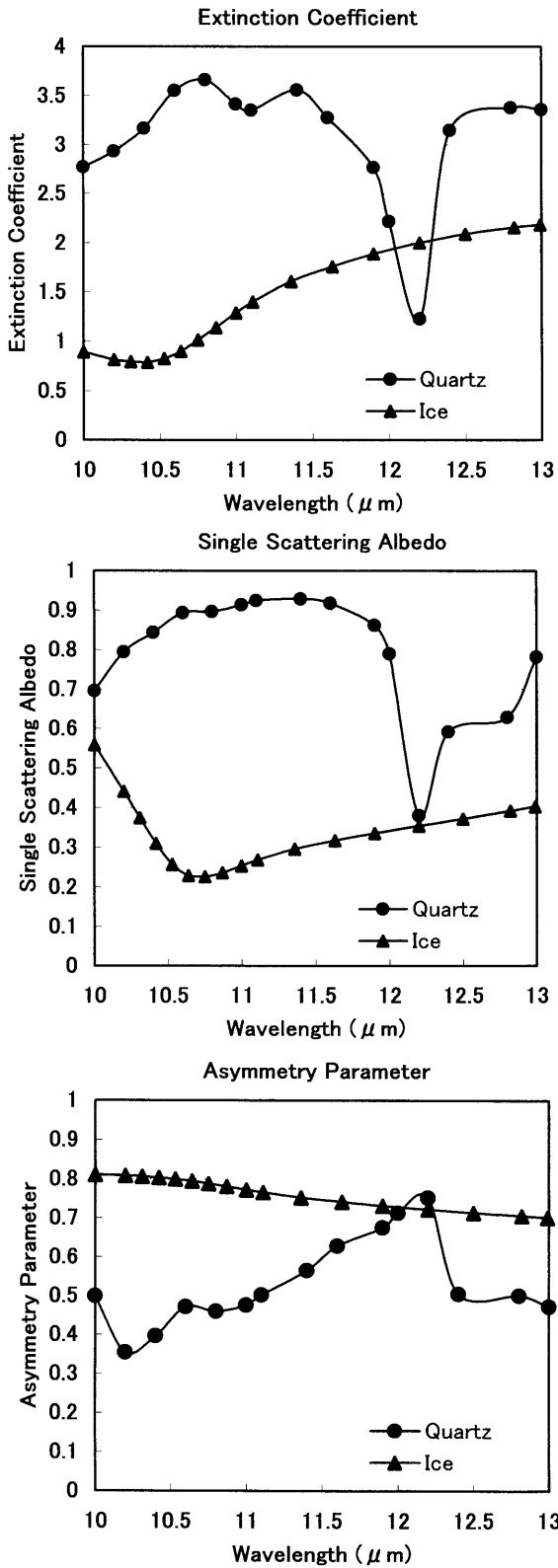


Fig. 3 The extinction efficiency factor Q_{ext} , asymmetry parameter g , and single scattering albedo ω for quartz (●) and ice (▲) as a function of wavelength. The modified- γ size distribution is used with $r_0 = 3 \mu\text{m}$, as described in Tokuno (1997).

extinction decreases with at wavelengths of 11.5 μm and 12 μm . For ice, the extinction increases with the wavelength in this region.

4. Model Calculations

Calculation of radiance observed by the satellite in the model is performed with a few assumptions: (1) the vertical profile of the atmosphere is the tropical, the midlatitude summer, and the midlatitude winter atmospheric model from Kneizys (1983), (2) the cloud base height is 10 km for the midlatitude summer and winter atmospheric models, and 14 km for the tropical model over the surface with a geometrical cloud thickness of 1 km, (3) the satellite view angle is zero degrees, and (4) the lowest layer of the atmospheric model is used instead of the earth's surface.

- 1) The values of scattering parameters with MTSAT, GMS-5, and NOAA-14 at wavenumber are given by interpolating the values of scattering parameters calculated in Chapter 3.
- 2) The optical cloud thickness at an interval of 5 cm^{-1} for the MTSAT, GMS-5 and NOAA-14 wavenumber is calculated for the specific total number of particles per unit of volume using the equation relating the factors for optical cloud thickness.
- 3) Satellite-observed monochromatic radiance is calculated at an interval of 5 cm^{-1} for the MTSAT, GMS-5 and NOAA-14 wavenumber using the altered equation for thermal radiance with the values obtained through steps (1) and (2).
- 4) Satellite-observed radiance for each channel is derived by combining the response (Fig. 1) with satellite-observed monochromatic radiance calculated in step (3), using the equation

for the sensor's observed response-weighted radiance.

- 5) Satellite-observed radiance is converted to brightness temperature using both the spectral response characteristics of the radiometer and the Planck function. The BTD between infrared window channels is then calculated.
- 6) Satellite optical cloud thickness for each channel is calculated by combining the response with the optical cloud thickness obtained through step (2).

Steps (2) to (6) are repeated until the value of the satellite optical cloud thickness reaches nine by increasing the specific total number of particles per unit of volume at an appropriate rate.

Temperature pairs and BTD values were simulated for MTSAT, GMS-5 and NOAA-14 along with the IR-1 temperatures for MTSAT and GMS-5 and ch. 4 temperature for NOAA-14 as a function of the mode of the particle radius (2, 3, or 5 μm) and the satellite cloud optical depth (0 - 9) for quartz and ice in the tropical atmospheric model (Figs. 4 and 5).

As expected, for quartz the negative BTD value is greatest with a mode of the particle radius of 2 μm , followed by 3 μm , and 5 μm . For increased or reduced optical depth, BTD decreases. As the mode particle radius grows larger, the negative BTD gradually decreases and becomes a positive value.

For quartz, the negative BTD value is greatest with MTSAT, followed by NOAA-14/AVHRR, and then GMS-5. For example, when the mode particle radius is 2 μm and satellite cloud optical depth is 3.0 in the tropical atmospheric model, the BTD value is -25 K for MTSAT, -22K for NOAA-14/AVHRR, and -16K for GMS-5.

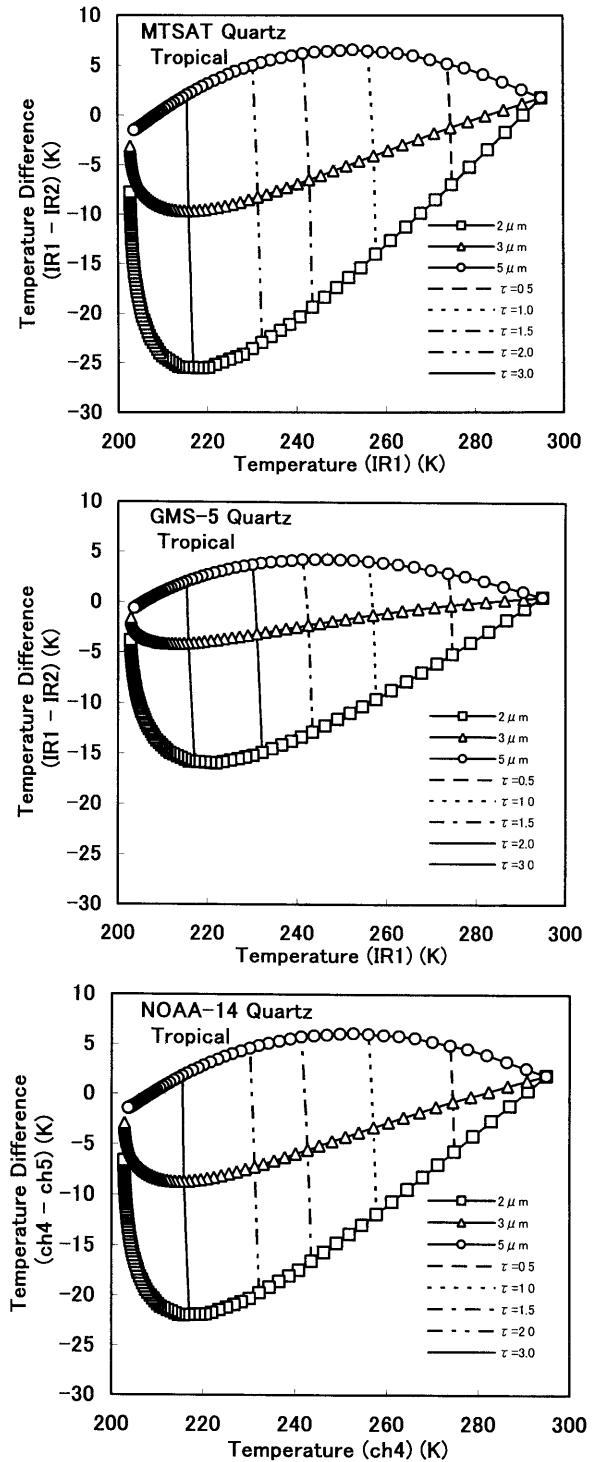


Fig. 4 Simulated temperature pairs and BTD values for MTSAT, GMS-5, and NOAA-14 AVHRR, along with IR-1 temperatures for MTSAT and GMS-5 and channel 4 temperature for NOAA-14 AVHRR as a function of the mode of the particle radius (2, 3, or 5 μm) and satellite cloud optical depth (0 - 9) for quartz in the tropical atmospheric model. The near horizontal curves represent different mode particle radiuses, and the near vertical curves the dependence of optical depth at IR-1 or channel 4 with the particle radius.

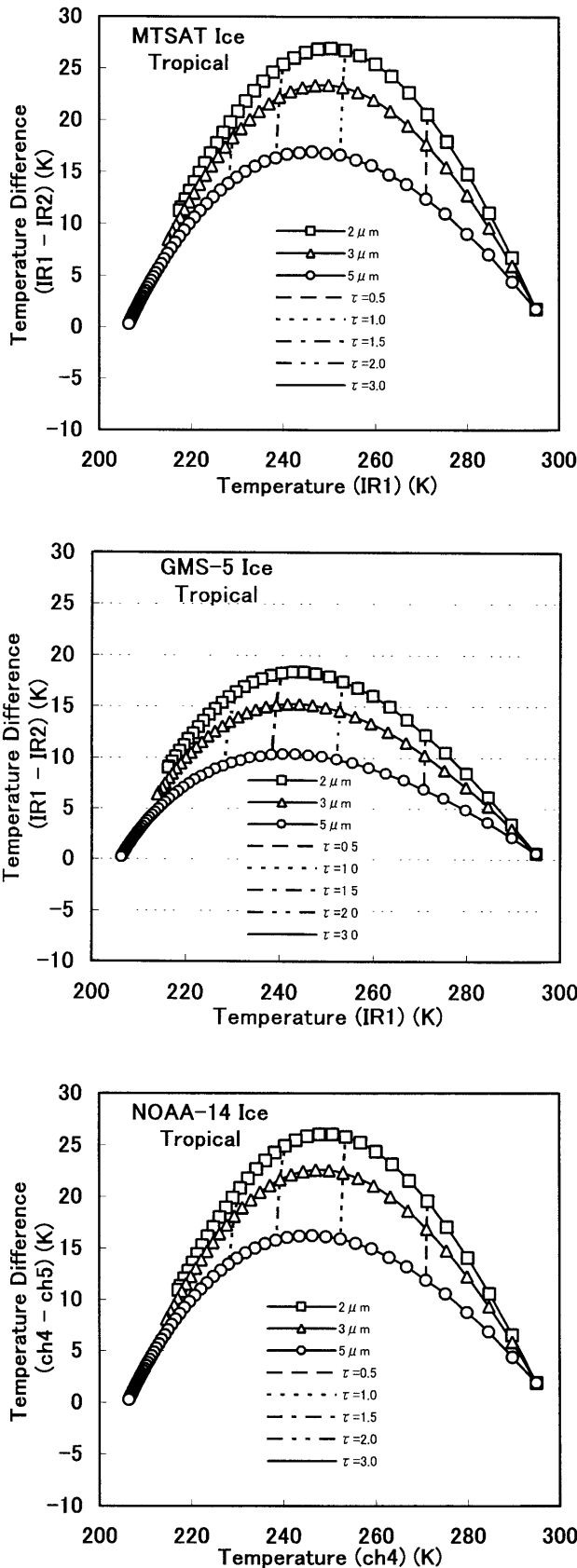


Fig. 5 The same as Fig. 4 for ice.

Thus, the BTD value for MTSAT is about 1.5 times as large as that for GMS-5. When the satellite cloud optical depth is zero, BTD value is positive, which is caused by different attenuation of the upwelling thermal radiance due to water vapor between the cloud and the earth's surface.

As shown with ice (Chapter 3), the tendency of forward extinction is opposite that in quartz, so the BTD tendency is opposite that of quartz, i.e., the positive BTD value is greatest with a mode of the particle radius of 2 μm, followed by 3 μm and 5 μm. Like quartz, the positive BTD value is greatest for MTSAT, followed by NOAA-14/AVHRR and GMS-5. For example, when the mode of the particle radius is 2 μm and optical depth is 1.5 in the tropical atmospheric model, the BTD value is 26 K for MTSAT, 25 K for NOAA-14/AVHRR, and 18 K for GMS-5. Thus, the BTD value for MTSAT is about 1.5 times as large as that for GMS-5.

To investigate the effect of the vertical profile of the atmosphere on BTD values, the same calculation has been performed in the midlatitude summer and winter atmospheric models for quartz (Figs. 6 and 7). The BTD value is greatest in the tropical model, followed by the midlatitude summer model, and the midlatitude winter model. The negative BTD value is greatest for MTSAT, followed by NOAA-14/AVHRR, and GMS-5 for the three atmospheric models. This result suggests that the BTD value for MTSAT among those of the three satellites is the most effective for discriminating between volcanic ash clouds and meteorological clouds, although the absolute BTD value is affected by cloud temperature and the earth's surface temperature.

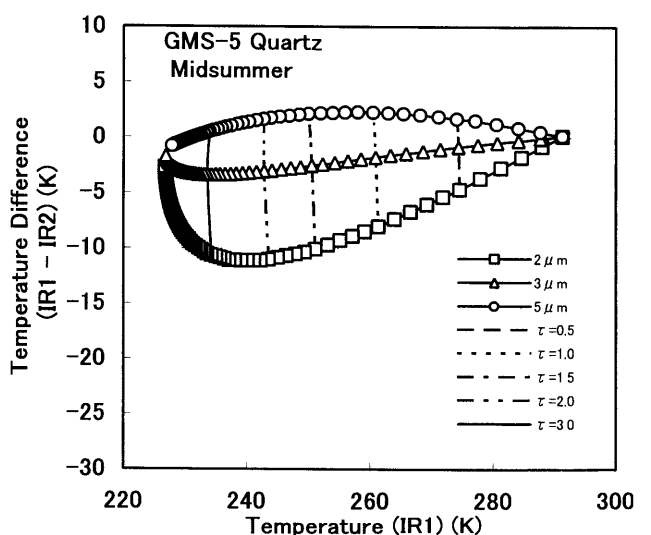
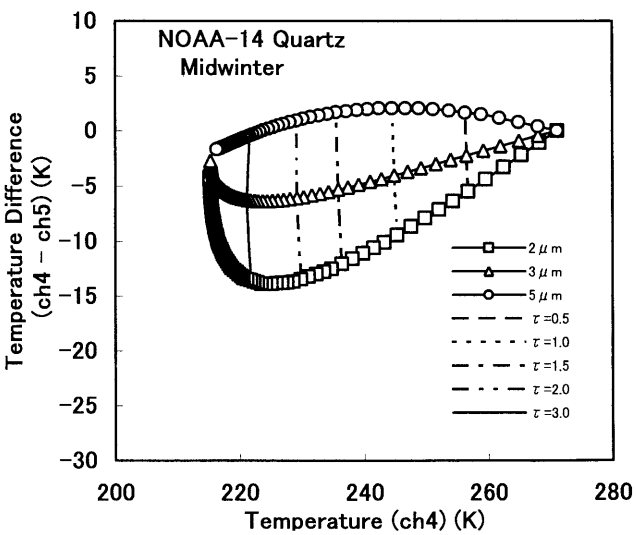
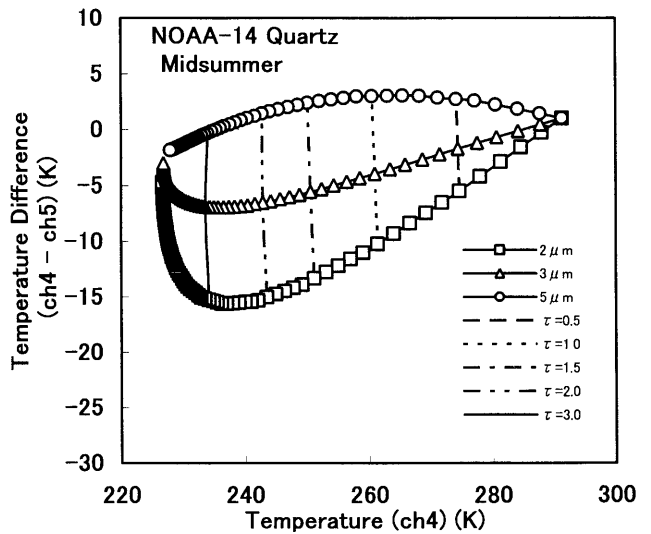
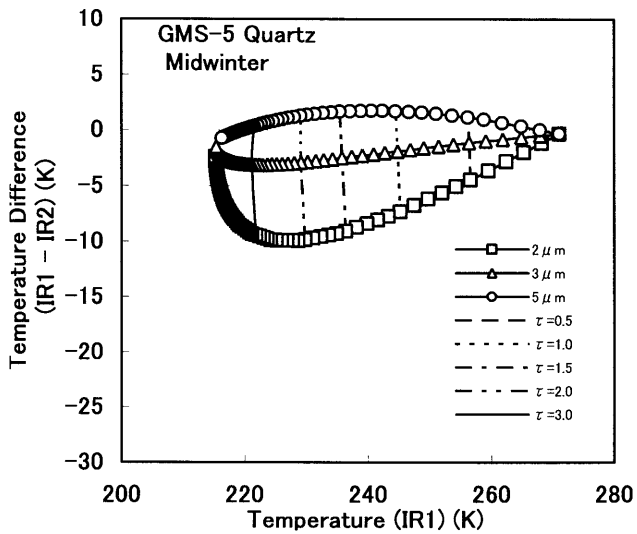
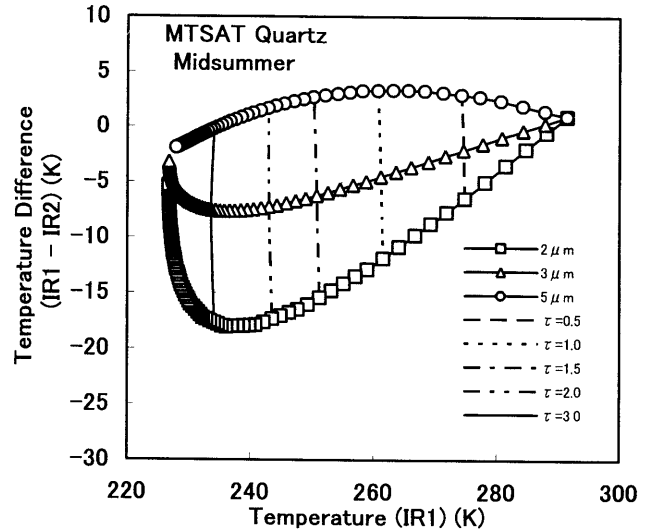
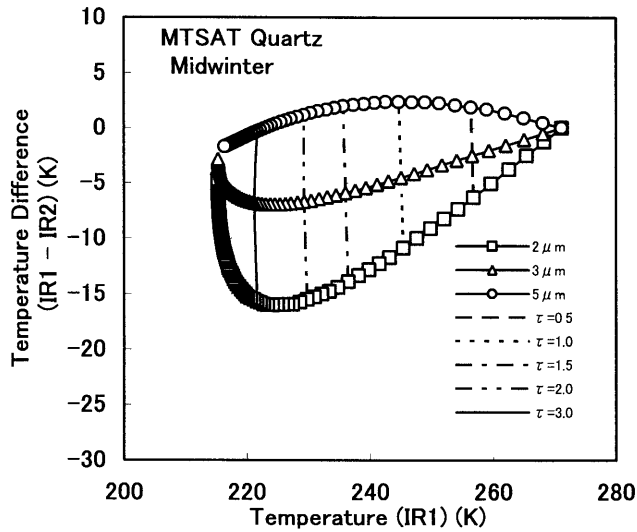


Fig. 6 The same as Fig. 4 for the midsummer atmospheric model.

Fig. 7 The same as Fig. 4 for the midwinter atmospheric model.

These results indicate that the use of MTSAT window channels for distinguishing volcanic ash clouds that include SiO_2 from ice/water clouds is more effective than using *GMS-5* due to improvements in the response functions of MTSAT's IR1 and IR2.

5. Conclusion

MTSAT has no overlap in spectral response functions for infrared sensors IR1 and IR2, which produces an increased BTDR for MTSAT compared to that for *GMS-5* and *NOAA-14/AVHRR*, based on results of a radiative transfer model. Therefore, MTSAT window channels IR1 and IR2 are more effective than *GMS-5* and *NOAA-14/AVHRR* channels for distinguishing volcanic ash clouds due to the spectral response functions. MTSAT data has thus been confirmed in MTSAT's further improvement of the detection of volcanic ash clouds when compared to *GMS-5*.

REFERENCES

- Ackerman, T.P., K.N. Liou, F.P.J. Valero, and L. Pfister, 1988: Heating rates in tropical anvils, *J. Atmos. Sci.*, 45, 1606 - 1623.
- Dave, J.V., 1968: Subroutines for computing the parameters of the electromagnetic radiation scattered by a sphere, IBM Palo Alto Scientific Center, 60 pp.
- Knelzys, F.X. et al., 1983: Atmospheric Transmittance/Radiance: Computer Code LOWTRAN 6, AFGL-TR-83-0187.
- Newell, R. E. and A. Deepak (Eds.), 1982: Mount St. Helens eruptions of 1980. Workshop Report, NASA SP-458, National Aeronautics and Space Administration, Washington, DC.
- Potts, R.J., 1993: Satellite observations of Mt. Pinatubo ash clouds, *Aust. Met. Mag.*, 42, 59-68.
- Prata, A.J., 1989: Observations of volcanic ash clouds in the 10 - 12 μm window using AVHRR/2 data, *Int. J. Remote Sensing*, 10, 751 - 761.
- Prata, A.J. and I.J. Barton, 1994: Detection and discrimination of volcanic ash clouds by infrared radiometry I: Theory, Proceedings of the First Volume, the First Int. Symp. on Volcanic Ash and Aviation Safety, U.S Geological Survey Bulletin 2047, 305 - 311, Thomas J. Casadevall (ed).
- Spizer, W.G. and Kleinman, D.A., 1961: Infrared lattice bands of quartz, *Phys. Rev.*, 121, 1324-1335.
- Takashima, T. and K. Masuda, 1987: Emissivities of quartz and Sahara dust powders in the infrared region (7-17 μm), *Remote Sens. Environ.*, 23, 51-63.
- Tokuno, M., 1997: Satellite observation of volcanic ash clouds, Meteorological Satellite Center Technical Note, 33, 29 - 48.
- Warren, S.G., 1984: Optical constants of ice from the ultraviolet to the microwave, *Appl. Opt.*, 23(8), 1206-1225.
- Whitten, R. C. (Ed.), 1982: The Stratospheric aerosol layer, Springer-Verlag, 152pp.

MTSAT窓チャンネル(赤外1と赤外2)による火山灰雲識別の可能性

徳野正己

GMS-5の赤外チャンネル1 (10.5 - 11.5 μm) 及び赤外チャンネル2 (11.5 - 12.5 μm) の輝度温度差は、火山灰雲では負に、自然の雲では正になり、火山灰雲と自然の雲の識別に利用されている。MTSATの赤外チャンネル1 (10.3 - 11.5 μm) 及び赤外チャンネル2 (11.5 - 12.5 μm) の応答関数がGMS-5と比較して大きく改善された。その改善に伴い、2つの熱赤外チャンネルデータによる火山灰雲と自然の雲を識別する能力の向上について放射モデルで計算した結果を基に調査した。放射計算は、半透明な雲モデルを用いて行われ、この雲モデルでは、球粒子で表面は均一で地球表面に平行な簡単な薄い平板の雲を仮定している。二つの赤外窓チャンネルの応答関数の違いにより生じる輝度温度差を評価するために、MTSAT, GMS-5, NOAA-14/AVHRRについて、輝度温度差を石英(火山灰雲)と氷(上層雲)の2例について計算した。大気の鉛直プロファイルは、熱帯大気モデル、中緯度帯夏大気モデル、中緯度帯冬大気モデルの3種類の大気モデルを使用し、雲底高度はそれぞれ14km, 10km, 10kmとし、雲の幾何学的厚さは1kmに設定した。粒径分布は改良された γ 分布を用い、光学的厚さは粒子の密度を変えることにより0から9まで変化させた。本研究で取り扱ったすべての場合について、輝度温度差は、MTSATの場合が最大で次にNOAA-14/AVHRRで最後がGMS-5であった。たとえば、熱帯大気モデルで粒径分布の粒子半径のモード値が2 μm , 光学的厚さが3.0の場合、輝度温度差はMTSAT, NOAA-14/AVHRR, GMS-5それぞれ-25K, -22K, -16Kであった。このように、MTSATデータはGMS-5と比較して火山灰雲の検出の能力が更に向上することを確認した。